Environmental Science: Atmospheres

ROYAL SOCIETY OF CHEMISTRY

PAPER

View Article Online
View Journal

Cite this: DOI: 10.1039/d6ea00039h

Unveiling the first two-year dataset on the atmospheric deposition of heavy metals in a southern Vietnam megacity: potential driving factors and ecological risk assessment

Ly Sy Phu Nguyen, *[ab] Le Quoc Hau,[ab] Vo Truong Gia Han,[ab] Tran Hoang Minh,[ab] Vo Thi Tam Minh,[ab] Tran Anh Ngan[ab] and To Thị Hien[ab]

Characterizing atmospheric deposition of heavy metals (HMs) through bulk sampling provides critical insights into environmental pollution patterns in fast-developing urban centers. Despite being a key economic hub in Southeast Asia (SEA), Ho Chi Minh City (HCMC) has received comparatively limited scientific attention regarding atmospheric deposition of HMs. This study reports the first 2 year (2023–2024) observation data of atmospheric deposition of HMs in HCMC. The volume-weighted mean (VWM) concentrations and deposition fluxes exhibit the same decreasing order: Zn (32.9 μg L^{-1}; 59 885 μg m^{-2} $year^{-1}$) > Mn (22.0; 40 151) > Cu (2.16; 3872) > Pb (1.52; 2839) > Ni (0.70; 1271) > Cr (0.42; 765.7) > V (0.19; 349.4) > As (0.09; 173.7). Bulk HM deposition fluxes increase during the rainy season as a result of enhanced rainfall, whereas the concentrations are lower (rainy < dry season), likely due to dilution effects. Seasonal variability in HM deposition is strongly modulated by the East Asian monsoon through its combined effects on air-mass transport pathways and rainfall-driven scavenging. Enrichment factor (EF) assessments, combined with principal component analysis (PCA), identified four major potential contributing factors on rainwater characteristics at HCMC: a mixture of non-combustion traffic sources and industrial sources, combustion sources, crustal sources, and meteorological influences. Ecological risk assessments indicated a low risk for most HMs (E_i < 30), in which Pb exhibits a high risk, accounting for 60% of the total potential ecological risk, implicating industrial emissions as the dominant contributor. This work provides the first quantitative assessment of atmospheric HM deposition in SEA, improving understanding of toxic metal inputs and supporting environmental management in rapidly urbanizing areas.

Received 20th March 2026
Accepted 7th April 2026

DOI: 10.1039/d6ea00039h

rsc.li/esatmospheres

Environmental significance

Atmospheric deposition of heavy metals (HMs) constitutes an important pathway of pollutant transfer to urban ecosystems, yet observational evidence remains scarce in Southeast Asia (SEA). This study presents the first comprehensive dataset of atmospheric HM deposition in a megacity in SEA, revealing pronounced seasonal variability that is dominated by abundant tropical monsoonal rainfall. Traffic- and industry-related emissions play a central role in governing the characteristics of atmospheric HM deposition. Despite lower mass contributions, Pb poses the highest ecological risk, accounting for approximately 60% of the total potential ecological risk index. These findings improve environmental risk assessment and provide a scientific basis for source-oriented pollution control in Southeast Asian megacities.

1 Introduction

Heavy metals (HMs), also known as potentially toxic elements, are a class of elements characterized by a high atomic mass and a density typically exceeding 5 g cm^{-3}.[1] Present naturally within the Earth's crust, HMs are introduced into the atmosphere *via* both geogenic processes, such as soil dust and sea spray, and anthropogenic sources, for example industrial emissions, fossil fuel combustion, vehicular exhaust, waste incineration, and mining activities.[2,3] With recognized toxicity even at low concentrations, HMs are regarded as persistent environmental pollutants of global concern because of their bioaccumulative nature and detrimental impacts on both ecological systems and human health.[4] In recent decades, rapid urbanization and industrialization (driven by intensified energy consumption, transportation, population growth, and construction) have significantly elevated atmospheric HM emissions in many regions across Asia, including China and Southeast Asia (SEA).[5,6]

[a]Faculty of Environment, University of Science, Ho Chi Minh City, Vietnam. E-mail: nlsphu@hcmus.edu.vn
[b]Vietnam National University, Ho Chi Minh City, Vietnam

HMs emitted into the atmosphere are typically adsorbed onto the surface of atmospheric aerosols, especially in the accumulation mode (0.1–1 μm), which facilitates their long-range transport over hundreds to thousands of kilometers.[6–8] Once released into the atmosphere, HMs can persist for days or weeks and are eventually eliminated from the atmosphere *via* dry and wet deposition, resulting in their transfer to terrestrial and aquatic ecosystems.[9,10] Atmospheric HMs in bulk deposition originate from both natural sources (*e.g.*, soil dust, volcanic activity, and biomass burning) and anthropogenic activities (*e.g.*, coal combustion, industrial manufacturing, transportation, and fertilizer).[5,11,12] Regarding spatial source contributions, both local emissions and long-range atmospheric transport of air pollution have been identified as significant contributors to HM deposition.[13–16] Wet deposition, precipitation-based removal *via* rainout and washout, is particularly efficient in humid subtropical regions and serves as a critical pathway for environmental HM loading.[16–18] Human activities have further intensified HM deposition across particular regions, including mining sites, transport routes, and central urban areas.[3,5]

The deposition flux of HMs is influenced by factors such as rainfall intensity, meteorological conditions, and the physicochemical properties of particles.[5,19] Wet deposition, driven by rainfall or snow, and dry deposition, occurring *via* gravitational settling or surface impact, are both significant pathways for removing atmospheric HMs.[13,17] Numerous studies have demonstrated that atmospheric deposition represents a key input of HMs into soils and agroecosystems.[3,5,20] For instance, atmospheric deposition contributes more than 50% of total inputs of toxic HMs, such as arsenic (As), cadmium (Cd), chromium (Cr), mercury (Hg), and lead (Pb), in Chinese croplands.[20,21] Unlike organic pollutants, HMs are non-degradable and possess high environmental persistence and bioaccumulative potential, posing chronic ecological and human health threats.[6,21]

Over the past decades, atmospheric deposition of HMs has intensified considerably across East Asia, particularly in China, where deposition rates have been reported to be approximately an order of magnitude higher than those observed in Europe.[5,6,17,22] Numerous regional investigations have revealed pronounced spatiotemporal variability in HM fluxes, driven by emission sources, meteorological conditions, and regulatory interventions.[5,23] For instance, deposition fluxes of Pb, nickel (Ni), and Cd in the Yangtze River Delta ranged from 1.11 to 27.3 mg m^{-2} $year^{-1}$ between 2015 and 2017,[12] while significant reductions in rural Beijing by 2020 reflected the efficacy of emission control policies.[23] In South Asia, air pollution hotspots such as Bangladesh have been shown to receive transboundary HMs input *via* monsoonal circulation systems.[13,14] In contrast, SEA, despite experiencing rapid urbanization and industrial growth and being strongly affected by the East Asian monsoon, observation studies on HMs deposition remain markedly limited in the literature. Most existing studies in Thailand, Malaysia, and Vietnam have focused on HM concentrations in particulate matter (PM), with limited data available on wet or bulk deposition fluxes.[6] The limited deposition measurements hinder assessments of the impacts of atmospheric HM pollution and highlight a significant knowledge gap in SEA.

As the most densely populated and urbanized city in Vietnam (*i.e.*, a SEA country), Ho Chi Minh City (HCMC) is increasingly burdened by air-quality issues arising from traffic emissions, industrial activities, and construction work.[24–26] Nevertheless, previous studies in HCMC have predominantly concentrated on HMs associated with road dust or PM_{10},[27–29] resulting in a notable gap in understanding of atmospheric HM deposition processes. To address this limitation, this study focuses on (1) quantifying the levels and estimating the fluxes of selected HMs in bulk deposition, (2) identifying the potential emission sources and controlling mechanisms responsible for HM deposition, and (3) exploring the potential ecological risk of HM bulk deposition. Beyond providing baseline observational data, this study aims to advance the mechanistic understanding of HM deposition under tropical monsoon conditions. By integrating seasonal flux analysis, trajectory clustering, and multivariate source apportionment, this work seeks to clarify how monsoon dynamics modulate both the magnitude and chemical composition of HM deposition in a rapidly urbanizing tropical environment, helping to support future efforts in air-quality management, risk assessment, and sustainable urban planning in the region.

2 Methodology

2.1 Site descriptions

In this study, bulk deposition samples were collected at the Nguyen Van Cu (NVC) campus of VNUHCM-University of Science (10.762°N, 106.680°E; Fig. S1). The sampling site lies in the central urban zone of HCMC, which is marked by dense population and heavy traffic activities.[25,26] The sampling was conducted on the rooftop of Block E (4th floor), about 25 m above ground level (a.g.l.). This elevation minimized immediate ground-level interferences while providing a representative height for monitoring urban atmospheric conditions. In addition, the bulk deposition sampler was installed at an open rooftop location with no significant obstructions within a 40 m radius, ensuring representative exposure to atmospheric inputs and minimizing potential interference from nearby structures. To enhance the reliability of rainfall data used for deposition flux calculations, the sampler was placed approximately 5 meters from the rain gauge, ensuring consistency and spatially representative rainfall measurements under field conditions.

Our sampling site is adjacent to Nguyen Van Cu Street, a major arterial road with consistently high traffic volumes, particularly during peak hours.[24,30] The surrounding environment comprises mixed land uses, including residential neighborhoods, commercial establishments, and small-scale industrial operations.[25,27,29] In addition to traffic-related emissions, the site's ambient air quality is influenced by nearby industrial sources within a 40 km radius. HCMC hosts several industrial parks and manufacturing clusters, such as Tan Binh, Binh Tan, and Tan Thuan, across both core and adjacent districts.[27] These zones accommodate a wide range of industries, including metal processing, plastic and rubber

manufacturing, textiles, electronics assembly, and battery production.[26,27] Emissions from these facilities, including combustion byproducts, HMs, and volatile organics, can be transported over varying distances and contribute to the atmospheric deposition observed at urban sites.[25,26,29]

HCMC is subject to a tropical monsoonal climate, dominated by two distinct seasonal wind regimes: the northeast (NE) monsoon prevailing during the dry season (December to April), and the southwest (SW) monsoon during the rainy season (May to October). These seasonal transitions influence both the direction and origin of air mass transport, along with the strength and spatial distribution of rainfall.[29,30] Over the course of the study period, the annual rainfall at the site (NVC) is more than 1800 mm, with the majority occurring during the rainy season. The mean atmospheric temperature is 28.4 ± 2.5 °C, and the mean ambient relative humidity is 79.7% ± 11.4%, consistent with the hot and humid climatic conditions typical of southern Vietnam.[25,28,30]

2.2 Bulk deposition sampling and analysis

Bulk deposition samples were obtained using a custom-designed open-field sampler placed on a stainless-steel stand to minimize splash contamination from surrounding surfaces (Fig. S2A).[31,32] The sampling setup consisted of a 15 cm diameter high-density polyethylene (HDPE) funnel mounted on a 1 L HDPE collection bottle (Fig. S2B). As the sampling device was kept open throughout the study period, bulk deposition samples represented a combination of wet and dry deposition.[5,23] Consequently, the measured fluxes cannot be partitioned into separate wet and dry components. Therefore, while rainfall clearly drives temporal variability, the contribution of dry deposition processes cannot be neglected and should be interpreted as embedded within the reported bulk fluxes. The concentrations of 8 HMs (zinc (Zn), manganese (Mn), copper (Cu), Cr, Ni, Pb, vanadium (V), and As) were quantified using Inductively Coupled Mass Spectrometry (ICP-MS) following the US EPA method 200.7 and the US EPA method 200.8. To investigate the potential sources of HM contamination in rainwater, additional elements (*i.e.* selenium (Se), antimony (Sb), calcium (Ca), and iron (Fe)) were quantified. Comprehensive descriptions of the sampling procedures, analytical methodologies, and QA/QC protocols are provided in SI Text S1.

2.3 Concentration and bulk deposition estimations

In this study, the monthly/yearly average concentration of HMs was taken as the volume-weighted mean (VWM) of HM concentrations; the calculation was as follows eqn (1):

$$C_{\mathrm{VWM}} = \frac{\left(\sum_i C_i \times V_i\right)}{\sum_i V_i} \quad (1)$$

where C_{VWM} is the concentration of the ith sample (μg L^{-1}), and V_i is the corresponding sample volume.

The weekly bulk deposition flux was calculated by multiplying the measured HM concentration in the rainfall by the corresponding weekly rainfall depth. Monthly and annual bulk deposition fluxes were estimated using the VWM concentrations and the cumulative rainfall for each respective period.[16,33]

2.4 The HYSPLIT model

The Hybrid Single Particle Lagrangian Integrated Trajectory (HYSPLIT) model, created by the National Oceanic and Atmospheric Administration (NOAA), has been extensively applied in various studies to simulate air-mass pathways before reaching sampling sites.[30,34] This model has been extensively applied in air pollution research both domestically and globally. In this study, 72 hour backward trajectories (BWTs) were generated with the HYSPLIT model, with input data from the Global Data Assimilation System (GDAS) at a spatial resolution of 1° × 1°. For each week with recorded rainfall, four BWTs were simulated at 00:00, 06:00, 12:00, and 18:00 (local time, UTC + 7), at an arrival height of 1000 m (a.g.l), corresponding to typical rainfall periods. 72 hour backward trajectories were selected to capture regional-scale transport pathways, while minimizing trajectory uncertainty that increases with longer simulation durations. An arrival height of 1000 m a.g.l. was chosen to approximate the lower free troposphere and typical cloud base levels, thereby better representing the air masses contributing to atmospheric scavenging rather than near-surface local turbulence. Cluster analysis was performed with the TrajStat software.[35]

2.5 The enrichment factor (EF)

The enrichment factor (EF) was used to assess anthropogenic contributions to HMs in atmospheric deposition by normalizing metal concentrations to a crustal reference element.[29,36] In this study, Fe was selected as the reference element due to its high crustal abundance and relatively low anthropogenic influence. Upper continental crust values from Querol *et al.*[38] were used as baselines. EF values were calculated according to eqn (2) and interpreted using established classification criteria (Table S2).

$$\mathrm{EF} = \frac{\left(\frac{C_i}{C_{\mathrm{Fe}}}\right)_{\mathrm{sample}}}{\left(\frac{C_i}{C_{\mathrm{Fe}}}\right)_{\mathrm{background}}} \quad (2)$$

2.6 Principal component analysis

Principal component analysis (PCA) is a multivariate tool commonly applied to determine and apportion potential sources or contributing factors of HMs in multiple environmental matrices, including bulk deposition.[38] In this study, PCA was employed as a receptor modeling approach, incorporating VARIMAX rotation to enhance interpretability, and was performed using SPSS software. This method reduces data dimensionality by extracting a smaller number of independent principal components (PCs) that effectively represent the original dataset.[26,36] The selection of PCs is based on eigenvalues greater than one (>1), following the Kaiser criterion. Additionally, Kaiser–Meyer–Olkin (KMO) values above 0.6 were used to

ensure sampling adequacy.[36] The explained variance and cumulative variance percentages were also computed to evaluate the contribution of each factor. VARIMAX rotation, an orthogonal rotation technique, was applied to maximize the variance of factor loadings and to ensure the derived components remained uncorrelated.[39]

2.7 Potential ecological risk (PER)

The Potential Ecological Risk Index (RI) is a widely recognized method for evaluating the potential ecological threats posed by environmental pollutants. This index is calculated using a specific set of formulas (eqn (3) and (4)) to quantify the potential harm that HMs could cause to ecosystems.

$$E_r^i = T_r^i \times \frac{C_s^i}{C_n^i} \quad (3)$$

$$\mathrm{RI} = \sum_{i=1}^{n} E_r^i \quad (4)$$

where E_r^i is the single-factor potential ecological hazard index, T_r^i is the toxic response factor of HMs, C_s^i is the concentration of HMs (Pb, Zn, Cu, Ni, Cr, and As) in rainwater, and C_n^i is the reference value. In this study, the reference values for HMs were based on the Vietnamese National Technical Regulation on Surface Water Quality, which represents the highest standard for surface water intended for domestic use. The classification criteria for ecological risk indices of HMs are presented in Table S2. In ecological risk assessments, the RI requires that pollutant classifications be tailored to account for both the specific type of pollutant and its concentration. The methodology was adjusted as per the proposed method by Ma *et al.*[5] It should be noted that the ecological risk assessment in this study is based on the dissolved (<0.45 μm) fraction of HMs measured in bulk deposition. Particulate-bound metals retained on filters were not quantified. As several elements, particularly Pb and Cr, may exist partly in less soluble particulate forms, the calculated RI reflects the potentially bioavailable fraction rather than total atmospheric HM input. Consequently, the reported risk levels should be interpreted as conservative, screening-level estimates of ecological threat. In addition, the bioavailability of the excluded particulate-bound fraction could change after deposition (*e.g.*, *via* soil acidification), potentially leading to a higher actual ecological risk than estimated.

3 Results and discussion

3.1 Rainwater HM concentrations

A total of 70 weekly samples were obtained between January 2023 and December 2024, representing around 97% of the total rainfall. Table S3 summarizes the characteristics of 8 HMs in bulk deposition samples collected in HCMC, with a relatively balanced distribution between 2023 (34 samples) and 2024 (36 samples). However, the temporal distribution in 2024 was uneven, as no samples were collected during February to April. The presence of all HMs indicates a pronounced accumulation of HMs in rainwater samples, implying the combined influence of multiple anthropogenic activities (*e.g.*, urban traffic, construction activities, and light-industry emissions). Among the 8 HMs, Zn exhibits the highest concentration (32.9 μg L^{-1}), indicating its dominant role in the HM deposition in the study area (Table S3). A similar trend (*i.e.* higher Zn concentrations than other HMs) is also observed in road dust and $PM_{2.0}$ samples in HCMC,[37,40] indicating the widespread presence and persistence of Zn across multiple environmental compartments, likely due to its association with traffic-related emissions and/or industrial sources, the primary sources of air pollution in HCMC.[29]

Furthermore, Fig. S3A illustrates the distribution of HMs observed in this study, indicating a pronounced disparity among individual elements. Zn and Mn are the most abundant species, comprising 59.4% and 31.9% of the total HMs, respectively. Cu and Pb form a secondary group of notable contributors (Fig. S3A). In contrast, other HMs (*i.e.*, Ni (1.3%), Cr (0.7%), V (0.3%), and As (0.2%)) account for only marginal proportions, suggesting their relatively minor roles in the overall HM profile. The relatively low As concentrations found in this study are consistent with earlier results from $PM_{2.0}$ and PM_{10} studies conducted in the same area.[29,40] This pattern is mainly driven by key emission sources in HCMC, with vehicular traffic and light industries playing the predominant role, whereas inputs from coal combustion in heavy industries are relatively limited.[25,37,40] In addition, the distribution of HMs exhibits notable seasonal variation between the rainy season (May–October; Fig. S3B) and the dry season (November–April; Fig. S3C). In both seasons, Zn and Mn are the dominant constituents, accounting for over 85% of the total metal concentrations. Both Zn and Mn show higher relative proportions in the rainy season (59.9% and 32.2%, respectively) compared to the dry season (58.1% and 31.8%, respectively). In addition, the contribution of Pb increases significantly in the dry season compared to the rainy season (Fig. S3B and C). These results suggest that the HM composition in rainwater was influenced by both seasonal emission source origins and meteorological conditions.

Weak but statistically significant negative correlations ($p < 0.05$ for all; Fig. S4) are observed between rainfall and HM concentrations, suggesting rainwater HM concentrations decreased with increasing rainfall depth (dilution effect). Similar observations have been recorded in previous research conducted in China,[41] Malaysia,[42] Korea,[43] and Taiwan.[16] A possible explanation for this phenomenon is that during the initial stages of rainfall, atmospheric HMs are efficiently scavenged by rainwater. As rainfall continues, the incoming rain becomes progressively less concentrated in pollutants, leading to a dilution of HM concentrations in the rainwater samples.[33,44,45]

Table S4 summarizes the concentrations of HMs in rainfall at HCMC and various sites in Asia. The concentration of Zn in the HCMC rainwater is 32.9 μg L^{-1}, representing a moderate level. This value is comparable to that observed in urban Kolkata, India (31 μg L^{-1}), yet remains considerably lower than the concentrations reported in urban regions of Bangladesh (177.7–535.6 μg L^{-1}), where elevated Zn levels have been attributed to

emissions from widespread brick kilns, industrial processes, and vehicular abrasion.[46,47] Furthermore, the Zn concentration recorded in this study is generally higher than those reported at coastal, remote, and suburban locations, except for Satkhira, Bangladesh, where higher values were observed (Table S4). The observed Mn concentrations in HCMC are elevated compared to those at most previously reported locations, with the exception of Jomsom, Nepal, a remote site where arid conditions, limited rainfall, and emissions arise from regional crustal dust and biomass burning.[48] The concentrations of Cu (2.16 μg L^{-1}) and Pb (1.52 μg L^{-1}) observed in HCMC are lower than those observed at most other urban areas, such as Singapore, and Dinajpur and Sylhet in Bangladesh (Table S4), suggesting a lower intensity of anthropogenic activities and/or influence from regional sources.[13] However, Cu and Pb levels in HCMC remain elevated compared to those in remote and suburban sites, such as Nam Co, China and Chuncheon, Korea (Table S4), suggesting notable urban influence. The highest recorded Pb concentration (6.5 μg L^{-1}) was observed at the coastal site in Satkhira, Bangladesh, likely influenced by historical Pb usage and ongoing industrial activities in this region.[13]

In contrast to other HMs, Cr concentration in HCMC (0.42 μg L^{-1}) is higher than at Sylhet (0.12 μg L^{-1}). This suggests that Cr in HCMC may originate from different localized sources, which are not as prominent in Sylhet. Moreover, Cr levels at several remote sites (*i.e.* Northeast Tibet, China (9.2 μg L^{-1}) and Jomsom, Nepal (2.66 μg L^{-1})) exceeded those reported in urban areas, indicating that natural sources, such as crustal dust or long-range transported air pollution, may also play a significant role in regional Cr deposition. The typical distribution of Cr highlights the importance of considering both anthropogenic and geogenic contributions in interpreting its atmospheric behavior. Ni in HCMC (0.7 μg L^{-1}) is among the lowest across all urban sites and even lower than in several remote and coastal sites in Bangladesh and Tibet, China (Table S4). Both V and As exhibit relatively low concentrations in HCMC rainwater, with mean values of 0.19 μg L^{-1} and 0.09 μg L^{-1}, respectively. These levels are not only lower than those observed at urban sites but also lower than at several remote locations (*e.g.*, Jomsom, Nam Co; Table S4). This trend suggests that V and As in HCMC are less influenced by local anthropogenic activities than other sites. Previous studies in HCMC also reported comparatively low As concentrations in road dust and PM samples relative to other Asian sites,[29,37] reinforcing this observation. The elevated levels of these elements in some remote regions likely reflect contributions from geogenic sources or long-range atmospheric transport.[41,43,49,50] In general, rainwater HM concentrations in HCMC exhibit distinct urban characteristics, with elevated Zn and Mn levels compared to most remote and coastal sites, reflecting urban emissions. Conversely, lower Cu, Pb, As, V, and Ni concentrations relative to other Asian cities suggest moderate anthropogenic influence, while Cr levels imply mixed local and regional natural sources. It should be noted that dilution effects may also contribute to concentration differences among sites; however, this factor could not be fully assessed due to limited rainfall data availability in the literature.

3.2 Bulk deposition fluxes of HMs

The bulk deposition fluxes of HMs collected in HCMC during 2023–2024 reveal substantial atmospheric inputs of HMs into the urban environment, with notable interannual variability (Table S3). HM deposition fluxes exhibit a slight downward trend in 2024 compared to 2023, which may be partly attributed to the decrease in HM concentrations in 2024 (Table S3). However, interpretation of interannual differences should consider the absence of sampling during February–April 2024. Based on sensitivity analysis, excluding equivalent months in 2023, the estimated interannual flux difference remains within ±15%, suggesting that overall trends are robust within observational uncertainty. Among all HMs, Zn consistently showed the highest bulk deposition flux, with an annual value of 59885.4 μg m^{-2} $year^{-1}$, emphasizing its dominant role in atmospheric deposition, likely attributed to traffic-related emissions and industrial activities (*i.e.*, metallurgical combustion sources[15]). Other HMs, including Cu, Pb, and Ni, exhibit considerable deposition fluxes of 3872.2, 2839.8, and 1271.6 μg m^{-2} $year^{-1}$, respectively, indicating sustained emissions from diverse anthropogenic activities. Although As is detected at lower fluxes (*i.e.*, 173.7 μg m^{-2} $year^{-1}$), its high toxicity, environmental persistence, and potential for bioaccumulation warrant significant environmental concern.

Rainfall exhibits a significant positive correlation with the bulk deposition fluxes of all HMs (R^2 = 0.28–0.71; Fig. 1), with Zn showing the strongest dependence, as rainfall explains 73% of its variability. This strong coupling indicates that wet deposition is the dominant pathway for Zn removal, with rainfall events substantially enhancing its atmospheric scavenging efficiency. Pb and As fluxes are also notably rainfall-driven, with more than 60% and 44% of their variability, respectively, explained by weekly rainfall. These findings are in agreement with previous studies in China,[23,51] which reported rainfall contributions of up to 70% to HM deposition flux variability. In contrast, relationships between deposition fluxes and rainwater HM concentrations are generally weak for most HMs (R^2 < 0.15 for Zn, Pb, As, V, and Cr), suggesting that their deposition was controlled more by rainfall intensity and frequency than by concentration (Fig. S5). The exception is Mn, which displays a moderate flux-concentration correlation (R^2 = 0.528), implying a greater influence from stable local emission sources, such as soil resuspension or industrial activities, where deposition was more directly tied to atmospheric abundance. The consistently stronger rainfall-flux correlations compared to flux-concentration relationships suggest that rainfall is a more robust predictor of HM removal from the atmosphere.

Despite exhibiting relatively moderate concentrations (Table S4), particularly when compared with several urban and industrial sites in China and South Asia, the annual deposition fluxes of HMs in HCMC are generally higher than those reported at many sites worldwide (Table S5). This apparent contrast between lower concentrations and higher fluxes is primarily attributable to substantial annual rainfall (~1855 mm), which markedly enhances the total deposition to local ecosystems. Such patterns indicate the importance of

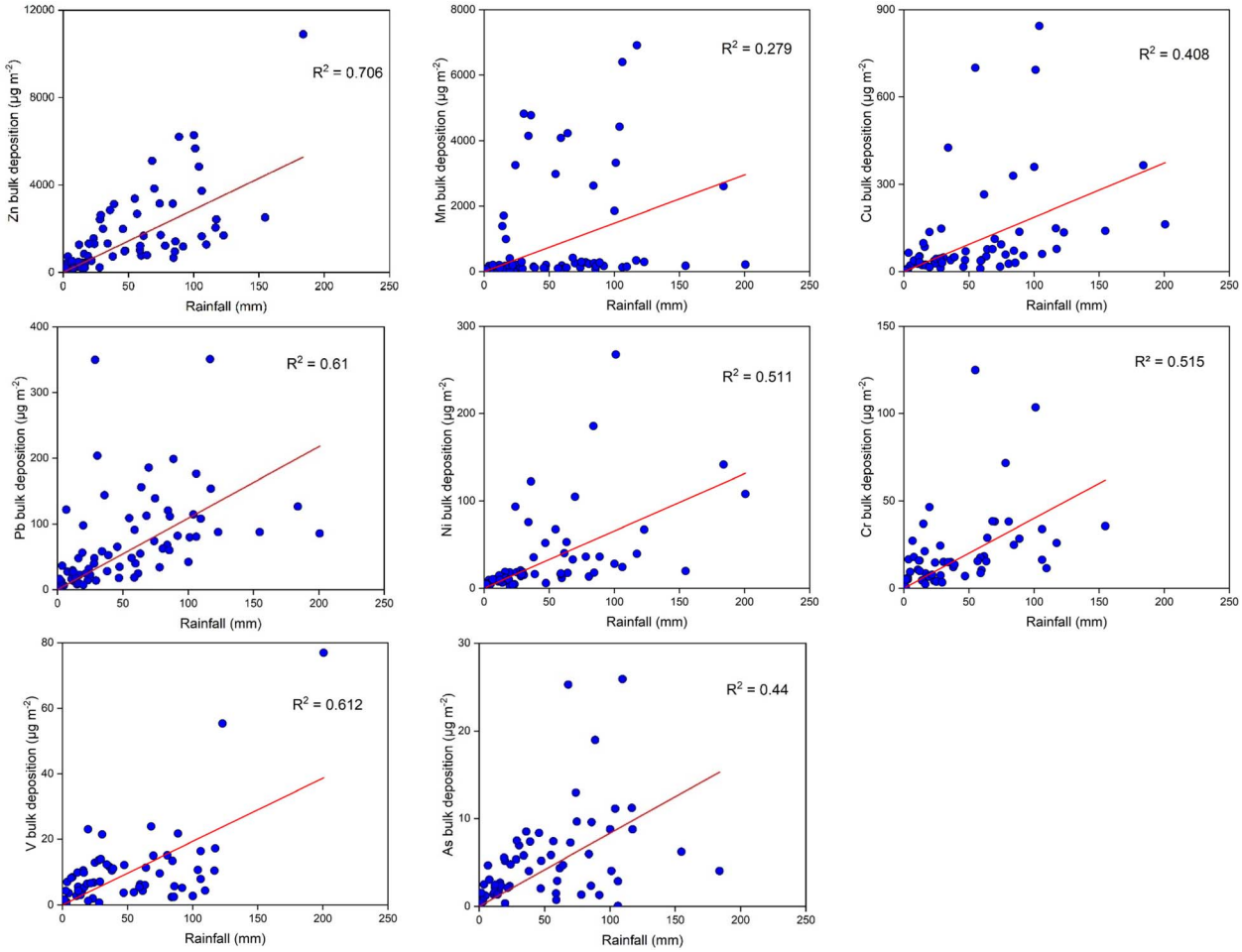

Fig. 1 Relationships between bulk deposition flux and rainfall amount.

considering precipitation volume in interpreting bulk deposition data, especially when comparing regions with differing climatic regimes. This effect is particularly evident for Zn (59 885.4 μg m^{-2} $year^{-1}$) and Mn (40 150.9 μg m^{-2} $year^{-1}$), two HMs associated with traffic-related emissions, abrasion from brakes and tires, and industrial processes. The deposition fluxes of Zn and Mn in HCMC far exceed those at remote Tibetan sites such as Nam Co, Southeast Tibet, and Lhasa, and even surpass levels in some urban Chinese locations (Table S5), despite lower precipitation concentrations (Table S4). Compared with highly polluted South Asian sites, however, the Zn and Mn fluxes observed in HCMC remain moderate. For instance, Sylhet, Bangladesh, recorded extremely high Zn and Mn fluxes (1 052 512 and 36 771.8 μg m^{-2} $year^{-1}$, respectively), largely driven by intense rainfall (5944 mm) and substantial local emissions.[13] Similarly, Dinajpur exhibited high Zn fluxes (938 335 μg m^{-2} $year^{-1}$) under moderate rainfall (1752 mm), indicating that both emission intensity and rainfall amount synergistically control deposition magnitudes.

For other HMs, As deposition flux at HCMC (173.7 μg m^{-2} $year^{-1}$) is markedly lower than values reported across Asia and especially China (Table S5). In Bangladesh, urban sites, such as Dinajpur (593.8 μg m^{-2} $year^{-1}$) and Sylhet (1820 μg m^{-2} $year^{-1}$), exhibited considerably higher fluxes. More strikingly, Chinese urban and remote sites displayed extremely high As deposition flux, reaching 4400 and 4800 μg m^{-2} $year^{-1}$ (Table S5), while remote regions, such as Lhasa (233 μg m^{-2} $year^{-1}$) and Satkhira (893.3 μg m^{-2} $year^{-1}$), also exceeded the HCMC level. These elevated fluxes could not be explained by rainfall amount, since annual rainfall in Chinese urban (~750 mm) and remote (~950 mm) sites was far lower than in HCMC (~1855 mm). Instead, they strongly reflect intense coal combustion, which is well recognized as the dominant source of atmospheric As in China.[5,52,53] The contrast in As concentration highlights that drove the extreme As burden observed at Chinese sites. The V flux in HCMC (349.4 μg m^{-2} $year^{-1}$) exceeds that of Jomsom, Nepal, which experiences very low rainfall (131.9 mm), and is comparable to those of some remote Tibetan regions (Table S5), suggesting contributions from petroleum combustion and possible long-range atmospheric transport.[49] In contrast, V flux in Singapore is substantially higher than in HCMC (Table S5), reflecting the combined effects of stronger emission intensities and higher annual precipitation (~2600 mm). Although abundant precipitation in HCMC enhances deposition, it is insufficient to offset the lower emission strength relative to Singapore, highlighting the coupled control of emissions and precipitation

on deposition fluxes. Pb fluxes at HCMC are markedly lower than those in coastal Bangladesh (*e.g.*, Satkhira: 12 549 μg m^{-2} $year^{-1}$; Cox's Bazar: 25 008 μg m^{-2} $year^{-1}$) and suburban China (*e.g.*, Dinghushan: 42 840 μg m^{-2} $year^{-1}$), reflecting a strong influence from local and regional anthropogenic sources.[13,54] On the other hand, Pb fluxes in HCMC remain more than 10 times higher than in Nam Co, Lhasa, and are comparable to those observed in multiple urban and remote sites in China (2500 and 2200 μg m^{-2} $year^{-1}$), indicating a pronounced urban influence (Table S5). In general, the relatively high Pb deposition at HCMC, despite lower or comparable concentrations (Table S4), could be explained by its abundant rainfall, whereas the extreme fluxes at Bangladesh sites primarily result from intense local emission sources.[13]

Cu and Ni deposition fluxes in HCMC (3872.2 and 1271.6 μg m^{-2} $year^{-1}$, respectively) are moderate compared with global observations (Table S5). For Cu, fluxes in HCMC are lower than those reported in Sylhet, Bangladesh (42 371 μg m^{-2} $year^{-1}$) and Dinajpur (16 562 μg m^{-2} $year^{-1}$), and exceed those observed at Tibetan remote sites (231–584 μg m^{-2} $year^{-1}$) and Beijing (560 μg m^{-2} $year^{-1}$). For Ni, HCMC fluxes are substantial, surpassing Beijing (530 μg m^{-2} $year^{-1}$) and Tibetan Plateau sites (97–171 μg m^{-2} $year^{-1}$), though they are still far lower than those recorded in Sylhet (90 673 μg m^{-2} $year^{-1}$) or Satkhira (6491 μg m^{-2} $year^{-1}$). On the other hand, Cr deposition fluxes in HCMC (765.7 μg m^{-2} $year^{-1}$) exceed those at all other sites, as reported in Table S5. Values at Sylhet, Cox's Bazar, Dinajpur, and Beijing were consistently lower, while remote Tibetan Plateau sites such as Nam Co (139 μg m^{-2} $year^{-1}$) and Lhasa (118 μg m^{-2} $year^{-1}$) showed only a fraction of HCMC levels. This dominance is particularly striking given the moderate Cr concentration in rainwater (0.42 μg L^{-1}, Table S4), emphasizing the role of abundant rainfall in enhancing fluxes. These results indicate that both local emissions and high rainfall contribute to the exceptionally high Cr deposition observed in HCMC. Overall, these results reveal that HCMC is subjected to substantial HM deposition driven by urban emission sources, with high rainfall acting as a critical enhancer of total deposition loads. Although absolute levels remain below those in South Asian cities, the cumulative fluxes to local ecosystems are nonetheless considerable.

3.3 Seasonal patterns

Fig. 2 illustrates the seasonal patterns of concentrations and bulk deposition fluxes of HMs in HCMC during the study period. A distinct seasonal contrast is evident, reflecting the strong influence of rainfall on deposition dynamics in HCMC. These pronounced seasonal contrasts are closely linked to the East Asian monsoon circulation.[16,30] During the rainy season (May–October), deposition fluxes of most HMs increase markedly, while their concentrations in rainwater tend to decrease (Fig. 2). This inverse relationship indicates that enhanced rainfall not only promotes efficient atmospheric scavenging but also dilutes the dissolved HM concentrations. Such dynamics emphasize the dual role of rainfall in regulating wet deposition through both washout processes and dilution effects.[16,23] The highest VWM concentrations for most HMs (except for Mn and Ni) occur in February, when limited rainfall (3.7 mm) reduces dilution and atmospheric cleansing (Fig. 2). In contrast, except for V, the lowest concentrations of all the HMs were recorded in

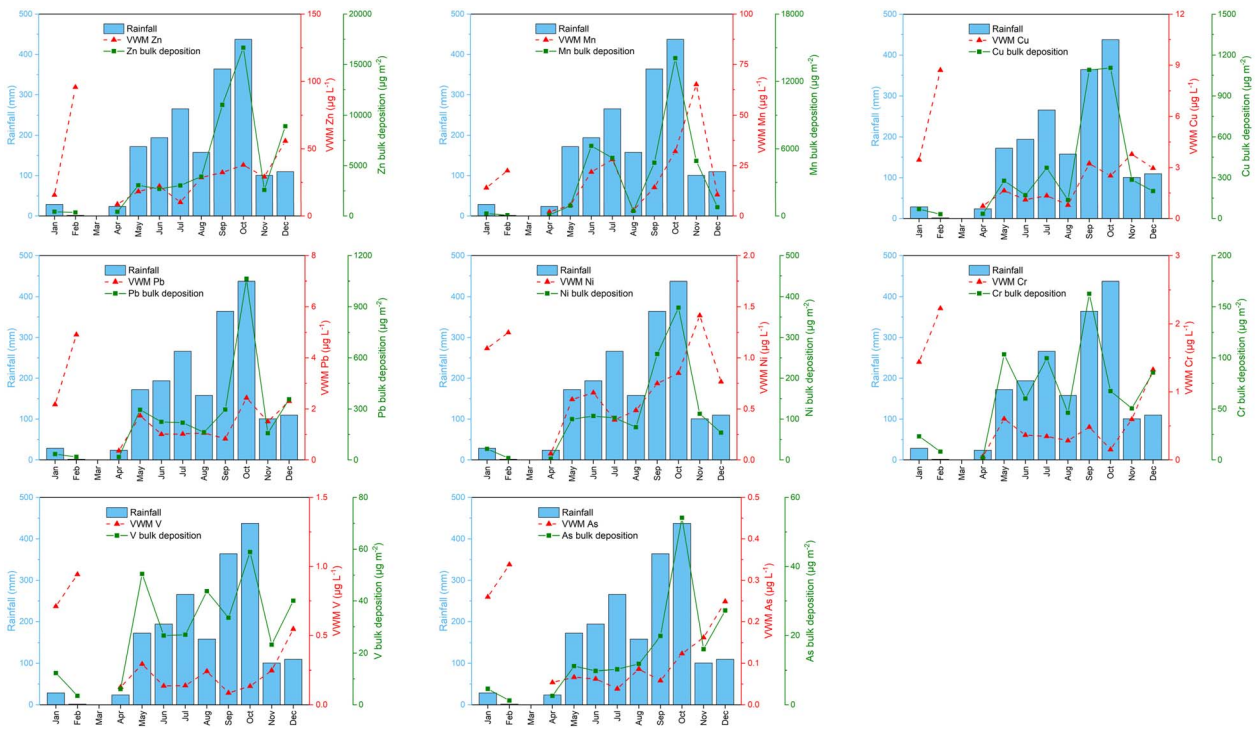

Fig. 2 Seasonal variations of HM concentrations, bulk deposition fluxes and rainfall at HCMC during the study period.

April, a period consistently associated with the annual minimum in air pollution over HCMC.[24,25,30,40] This reduction is influenced by the dilution effect of clean marine air masses transported from the open ocean.[24,29,55] The maximum bulk deposition fluxes of all HMs were recorded in the rainy season, with particularly high values in October, when rainfall is most intense. This divergence highlights the important role of rainfall in shaping the seasonal pattern of HM deposition, whereby heavy rainfall enhances deposition fluxes through effective washout, while simultaneously diluting dissolved HM concentrations in rainwater.

Mn generally followed this seasonal pattern, suggesting that rainfall was a key factor in removing Mn-containing aerosols and transporting Mn to the surface.[5,56] However, despite relatively substantial rainfall in August (~158 mm), neither Mn concentrations nor fluxes decrease significantly compared to other rainy months. A year-to-year comparison confirms this stability, as VWM Mn concentrations were 2.54 μg L^{-1} in August 2023 and 3.17 μg L^{-1} in August 2024, with rainfall amounts of 133.9 and 182 mm, respectively. This stability may result from redox transformations and leaching saturation. Under oxygen-rich conditions, Mn is readily oxidized to less soluble Mn(III/IV) oxides, such as MnO_2, which reduces its solubility in rainwater.[57] In addition, once the readily soluble Mn fraction is depleted earlier in the wet season, subsequent rainfall events contribute little additional Mn, consistent with leaching saturation reported in field studies.[58]

Other HMs show distinct seasonal characteristics. V exhibits notable monthly variability in rainwater concentrations, with higher values observed during dry months and lower values during the peak rainy months (Fig. 2). This pattern suggests that atmospheric dilution and rainfall scavenging play important roles in shaping its seasonal behavior. The elevated levels in the dry season may be attributed to the accumulation of combustion-related emissions, particularly from heavy fuel oil and industrial processes, under limited washout conditions. By contrast, enhanced rainfall in the wet season facilitates efficient removal of V from the atmosphere, leading to lower measured concentrations. Zn consistently dominates among all HMs, contributing more than half of the total deposition, with a pronounced seasonal contrast (Fig. 2). Concentrations peak in February, reflecting pollutant accumulation during the dry season when atmospheric washout is minimal. In contrast, fluxes reach their maximum during the wet season, particularly during September–October, when abundant rainfall enhances the scavenging of Zn from the atmosphere. Zn is widely recognized as a tracer of traffic-related emissions, including tire wear, brake abrasion, and industrial additives.[37,52,59] Its high solubility in rainwater further facilitates efficient washout during rainfall events, which explains the marked increase in wet-season deposition fluxes.[5,60,61] Compared to less soluble metals, such as Cr and Pb, Zn thus not only dominates in terms of concentration but also contributes disproportionately to the total deposition load.

Cu and Pb exhibit relatively stable concentrations throughout most of the sampling months, with only minor fluctuations, except for a pronounced increase in February when both elements reached their highest levels. Despite these elevated concentrations in February, the deposition fluxes of Cu and Pb are not high in that period but instead peaked in October, coinciding with the rainy season. This pattern highlights the dominant influence of rainfall volume on deposition fluxes, as abundant rainfall in October facilitates more effective removal of these elements from the atmosphere, resulting in larger fluxes irrespective of concentration levels. In contrast, Cr displays a more pronounced seasonal variation (Fig. 2). Concentrations of Cr are higher during the dry months, while the deposition flux reached a maximum in September. This peak is driven by the combined effects of relatively elevated concentrations and substantial accumulated rainfall, leading to enhanced atmospheric deposition flux of Cr. Such differences between Cu, Pb, and Cr imply a complex interplay between emission intensity, atmospheric processes, and precipitation in shaping the temporal variability of HM deposition in HCMC.

In general, the seasonal patterns of HM concentrations and deposition fluxes in HCMC highlight the strong influence of the tropical monsoon climate on atmospheric processes. The clear contrast between the dry and rainy seasons indicates that precipitation is the primary driver shaping HM deposition dynamics. Although the highest concentrations of most HMs are recorded in the dry months, the greatest bulk deposition fluxes occur during the rainy season, particularly in October when rainfall is most intense. This divergence emphasizes that rainfall not only dilutes HM concentrations in rainwater but also enhances their removal from the atmosphere, thereby increasing the overall deposition load to terrestrial and aquatic environments. The contrasting patterns of concentrations and fluxes illustrate the complex interactions between meteorological factors and anthropogenic emissions in determining the chemical composition of rainwater. To further clarify the contribution of specific emission sources to these patterns, a source apportionment analysis was conducted, as presented in the next section.

3.4 Source apportionment

3.4.1 BWT analysis. Clustering of backward trajectories (BWTs) is employed to elucidate the variability in HM concentrations observed in HCMC (Fig. 3). The trajectories reveal the combined influence of both the NE and SW monsoon systems, transporting air masses across a mixture of continental and oceanic pathways. Based on trajectory patterns during the study period, 4 major clusters are identified, each representing different transport characteristics and, consequently, distinct HM profiles (Table S6 and Fig. 3).

Clusters 2, 3, and 4, which collectively represented 65% of the total trajectories, are predominantly linked to southwesterly flows passing over vast marine regions in the Indian Ocean, Bay of Bengal, and Gulf of Thailand. The extended transportation of these air masses over relatively clean oceanic environments likely allowed for substantial dilution and deposition of contaminants during transport, thereby reducing the effect of long-range anthropogenic transport.[25,30,62] As a result, the chemical signature of rainfall during these periods is more

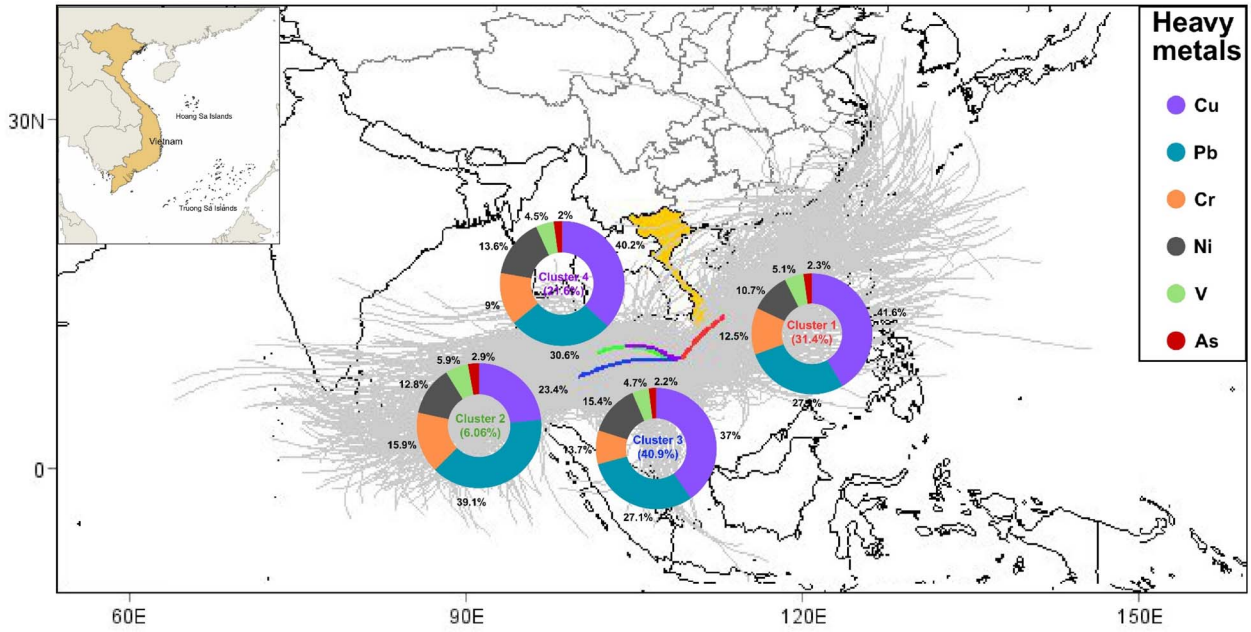

Fig. 3 Cluster analysis result and distribution of the selected HMs in HCMC during the study period. The gray lines represent the BWTs associated with rainy weeks.

strongly governed by local contributions. In contrast, cluster 1, accounting for 35% of all trajectories, is associated with inland pathways originating from northern and central Vietnam and partly influenced by continental flows from East Asia. Unlike the maritime clusters, these inland pathways offer less opportunity for dilution, thereby favoring the gathering of pollutants along the transport route.

The concentration profiles of HMs across the 4 clusters exhibit consistent dominance of Zn and Mn but also marked differences in the magnitude and distribution of HMs. In all clusters, Zn ranked first, followed by Mn, indicating their pervasive contribution to atmospheric deposition chemistry in HCMC. However, the relative abundance of secondary metals, such as Cu and Pb, varied considerably, leading to distinct chemical signatures among clusters (Table S6). For all clusters, the presence of Pb further highlights the persistent influence of residual sources despite the global phase-out of lead gasoline, reflecting localized industrial activities (Fig. 3). Similarly, Cu enrichment indicates substantial traffic-related abrasion processes in densely populated areas of HCMC (Fig. 3). Thus, the predominance of these HMs implies the dominant role of local emissions under the influence of cleaner maritime air masses. Cluster 1 shows the highest total concentration, with Zn and Mn contributing nearly 88% of the mass (Table S6). Cu is also elevated, nearly double the levels recorded in clusters 2 and 3, while Pb remains moderate. In contrast, results from Table S6 indicated that cluster 3 presents the lowest total concentration, characterized by substantially reduced Mn and Cu, while Zn also declines relative to cluster 1. This contrast suggests that cluster 3, dominated by cleaner southwesterly air masses, is more strongly influenced by dilution during oceanic transport, resulting in uniformly lower concentrations of all metals. Cluster 2 has Zn (44.6 μg L^{-1}) levels comparable to those of cluster 1 but slightly reduced Mn, while cluster 4 exhibits the lowest overall HMs concentrations among the clusters (Table S6).

Overall, cluster 1 and cluster 3 represent the two extremes of concentration levels, with cluster 1 reflecting the accumulation of pollutants under inland trajectories and cluster 3 highlighting the effect of long-range dilution over marine pathways. The intermediate patterns of clusters 2 emphasize the complex interplay between common Zn–Mn dominance and variable enrichment of Cu under specific transport regimes.

3.4.2 Enrichment factors. Table S2 presents the EF values of HMs in rainwater observed in this study. According to Table S2, a wide range of enrichment levels was obtained for HMs in our study. V showed a relatively low enrichment level, with an average EF of 3.64, suggesting a moderate influence by local anthropogenic activities (Table S7). In contrast, Cr (19.3) and Mn (22.0) exhibited severe enrichment, indicating the contribution of urban emission sources. Much higher EF values were observed for Ni (44.6), Cu (90.2), Zn (307.1), As (57.9), and Pb (73.7), suggesting strong enrichment relative to crustal abundance. Among these elements, Zn exhibited the highest EF, followed by Cu and Pb, highlighting the significant impact of anthropogenic activities.[63] The elevated enrichment levels are commonly associated with traffic-related emissions, fuel combustion, and urban industrial activities, which are major emission sources in Ho Chi Minh City.[26,29,37]

Overall, the EF results indicate that most elements are strongly influenced by anthropogenic inputs rather than purely crustal sources. The evident enrichment of Ni, Cu, Cr, Mn, Zn, As, and Pb suggests the presence of multiple urban emission sources. To further distinguish and identify these potential sources, PCA was subsequently applied.

3.4.3 PCA studies. Table S8 illustrates the correlations among metals in rainwater samples obtained throughout the study period, suggesting that they share common sources.[27] Specifically, Ni, Cu, Cr, and Mn show very high positive correlations ($r = 0.76$–0.84), reflecting significant impacts from on-road traffic and associated non-exhaust emissions (*e.g.*, brake and tire wear).[26,27] Furthermore, correlation of As with other metals also indicates a combination of multiple sources as moderate correlations with Fe ($r = 0.54$), Zn ($r = 0.59$), Pb ($r = 0.76$), and V ($r = 0.67$) ($p < 0.01$), highlighting the combined effects of fossil fuel combustion and smelting activities.[23,64] On the other hand, the analysis also shows significant contributions from natural sources. Ca shows only weak positive correlations with anthropogenic metals such as As, Pb, and Se, suggesting a clear contribution from crustal inputs (Table S8). To identify and separate these contributions more precisely, we performed PCA. The PCA was conducted to identify the major factors contributing to the variation of HMs in HCMC rainwater during 2023–2024 (Table 1). A Kaiser Meyer Olkin (KMO) value of 0.733 indicated that the dataset is suitable for PCA. Four principal components (PC) are extracted, explaining 73.3% of the total variance, indicating a well-structured dataset (Table S9).

The first PC (PC1), which accounts for 39.5% of the variance, exhibits high positive loadings for Ni (0.88), Cu (0.84), Cr (0.78), and Mn (0.76). These elements are widely recognized as tracers of urban and traffic-related activities.[29,37] Strong correlations, particularly between Cu–Ni ($r = 0.79$) and Cu–Cr ($r = 0.81$) ($p < 0.01$, Table S8), highlights the likelihood of common emission sources. In the context of Ho Chi Minh City (HCMC), traffic emissions represent a dominant contributor, especially given the large number of two-stroke motorbikes (>450 000 (ref. 65)), which release Ni, Cu, and Mn through incomplete fuel combustion, lubricant additives, and mechanical wear processes. A previous study in HCMC also identified tire wear, fuel combustion, and metallurgical activities as significant sources of Ni and Cu in PM_{10}.[29] The observed Cu–Cr and Ni–Cr associations ($r = 0.84$) further suggest the combined impact of non-exhaust vehicle emissions (*e.g.*, brake and tire abrasion) and localized industrial sources.[29,37] The strong Mn loading in PC1, together with its significant correlation with Cu ($r = 0.82$, $p < 0.01$), implies contributions from traffic activities. Taken together, PC1 can be viewed as representing factors relating to non-combustion traffic and industrial sources, reflecting the strong imprint of urbanization on atmospheric deposition.

Table 1 PCA of HMs in bulk deposition in HCMC

	Principle component (PC)			
	1	2	3	4
Ni	0.884	0.179		
Cu	0.840	0.127		
Cr	0.784	0.246		
Mn	0.761		0.367	
Sb	0.745	0.312	−0.350	
As	0.195	0.931		0.175
Fe		0.925	0.214	
Pb	−0.117	0.825		−0.110
Zn	0.190	0.742		
V	0.355	0.709		0.139
Se	0.287	0.580		
Ca			0.880	
Rainfall	−0.197	−0.149	−0.254	−0.644
Temperature		0.216	−0.157	0.830

The second principal component (PC2), explaining 15.5% of the variance, is dominated by As (0.93), Fe (0.92), Pb (0.82), Zn (0.74), and V (0.71). These elements are commonly linked to industrial activities, including metallurgical processes, fossil fuel combustion, and shipping emissions.[3,40,66] Moderate correlations between Zn and Pb ($r = 0.52$) suggest shared origins, possibly from local industrial emissions and/or traffic emissions. Similarly, the Fe–As association ($r = 0.54$) revealed these HMs originated from similar anthropogenic activities, probably combustion of fossil fuel.[23,29,64,66] Therefore, PC2 is mainly attributed to combustion-related sources.

The third principal component (PC3), accounting for 9.93% of the variance, is characterized by a single dominant loading of Ca (0.88). Unlike the anthropogenic HMs in PC1 and PC2, Ca exhibits weak and statistically insignificant correlations with other variables ($p > 0.05$), indicating a predominantly natural origin. Ca is widely regarded as a marker of crustal and resuspended dust, originating from soil particles, road dust, and construction debris.[37,67,68] Its enrichment in PC3 is consistent with inputs from wind-blown dust and urban land disturbance, processes that are particularly relevant in rapidly developing cities such as HCMC. The clear separation of Ca from anthropogenic HMs further supports its geogenic nature. Similar findings have been reported in other Asian urban environments, where Ca serves as a reliable tracer of natural mineral dust contributions.[66,68,69]

The fourth component (PC4), explaining 8.32% of the variance, reflects the role of meteorological factors, primarily temperature and rainfall, in modulating the characteristics of rainwater in HCMC. Such influences are particularly critical in tropical climates such as HCMC, where high rainfall intensity and seasonal variability strongly affect atmospheric scavenging processes.

Overall, the PCA results highlighted the complex contribution factors in rainwater at HCMC. The distinct clustering of HMs in anthropogenic traffic-industrial groups (PC1 and PC2), along with the contributions of natural crustal inputs (PC3), and meteorological influences (PC4), suggested the multifaceted drivers of rainwater chemistry in a rapidly urbanizing megacity. By disentangling the roles of urban activity, industrial development, natural dust inputs, and meteorological controls, this multivariate analysis provides a scientific foundation for improving air quality management and pollution control in tropical urban environments.

3.5 Ecological risk assessment

The ecological risk assessment of HMs in atmospheric deposition at HCMC reveals an evident divergence between measured

concentrations and the associated ecological hazards. As illustrated in Fig. 4, the E_i of Pb, Zn, Cu, Ni, Cr, and As all remain below the threshold of 30, classifying them as low ecological risk (Fig. 4A). When considered cumulatively, Pb accounts for approximately 62.9% of the total ecological risk (Fig. 4B), followed by Zn (24.8%) and Cu (7.3%), while the contributions from Cr, Ni, and As are negligible (<3%). This distribution identifies Pb as the dominant ecological risk factor in HCMC rainwater.

An important observation emerges when comparing deposition concentration and ecological risk. Zn displays the highest concentration among the investigated HMs, reflecting its strong anthropogenic presence in the urban atmosphere. Despite this abundance, Zn contributes relatively little to the overall ecological risk. This can be explained by the low T_r^i assigned to Zn in the risk model, which greatly diminishes its weighted ecological risk contribution. In addition, Zn is an essential micronutrient for plants and organisms, and while excess Zn can cause phytotoxicity or disturb microbial soil communities, its ecological hazard per unit mass remains much lower than that of Pb.[70] On the other hand, Pb shows a high ecological risk, despite having lower absolute concentrations than Zn. This reflects the strong persistence of Pb in the environment, lack of biological function, high mobility in acidic soils and aquatic systems, and its well-documented ability to bioaccumulate and biomagnify through trophic chains.[71,72] Pb exposure disrupts enzymatic processes, interferes with photosynthesis, and causes neurotoxicity in higher organisms, even at trace levels. Thus, the contrast between Zn and Pb highlights the critical role of toxicity weighting factors in risk models, and deposition magnitude alone can not be used as a surrogate for ecological threats. In addition, the results from HCMC are consistent with national-scale assessments across China. For example, Ma *et al.*[5] reported a comprehensive RI of 11.8 for bulk deposition across 31 sites, with the order of ecological risk contribution Cd > Pb > As > Ni > Cr > Se. In China, Cd emerged as the dominant risk factor, largely attributed to coal combustion and smelting emissions, whereas Pb remained the second-highest contributor.

The cumulative PER value is driven almost entirely by Pb (Fig. 4B). This finding has important implications for environmental management. Given that Pb pollution is difficult to remediate once deposited, strict emission controls should be prioritized. Measures such as enhanced regulation of industrial Pb sources, phasing out informal recycling activities, and mitigation of traffic-related Pb emissions are potentially needed. Although Zn exhibits a lower relative risk, its high deposition flux suggests the potential for long-term accumulation in soils and aquatic ecosystems. Prolonged enrichment may gradually shift Zn from a low to a moderate ecological concern, particularly under conditions of acidification or nutrient imbalance, which can enhance Zn bioavailability.

In summary, the ecological risk of HMs in HCMC is characterized by a disproportionate dominance of Pb, reflecting its high toxicity, environmental persistence, and anthropogenic sources. Zn, despite being the most abundant HM in deposition, exerts only a secondary ecological influence due to its lower toxicity coefficient and partial biological utility. This

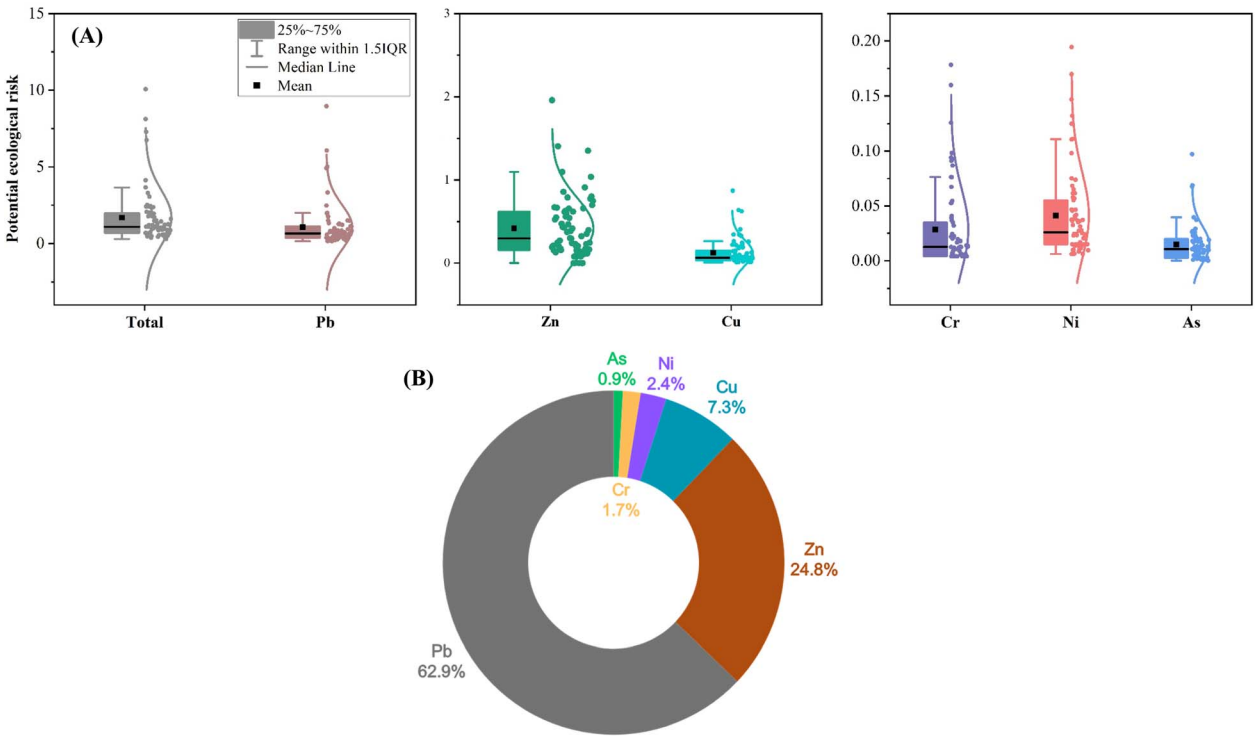

Fig. 4 Potential ecological hazard assessment of HMs in atmospheric bulk deposition in HCMC: (A) for each HM and (B) relative contribution to the total.

difference highlights the importance of adopting risk-based approaches over concentration-based methods in air pollution management. In the context of accelerating urbanization and industrial growth in HCMC, targeted reduction of Pb emissions should be considered a policy priority to safeguard ecosystem health. The ecological risk assessment in this study is based on the deposition of dissolved HMs, which reflects the more bioavailable fraction but may underestimate total HM loading. Inclusion of particulate-bound metals in future studies would allow for a more comprehensive ecological evaluation.

4 Conclusion

This study provides a comprehensive dataset on atmospheric deposition of HMs in HCMC, a rapidly urbanizing megacity in southern Vietnam. The results indicate that both HM concentrations and deposition fluxes are strongly influenced by seasonal rainfall patterns. Concentrations are generally lower during the rainy season due to dilution, whereas deposition fluxes are markedly enhanced by abundant precipitation. Zn shows the highest concentration, with a VWM of 32.9 μg L^{-1} and an annual deposition flux of 59 885 μg m^{-2} $year^{-1}$. Although absolute concentrations are moderate compared with several Asian urban sites, the cumulative deposition fluxes in HCMC are higher than at other locations worldwide due to high annual rainfall exceeding 1800 mm. The EF results indicate that most of the investigated elements are predominantly influenced by anthropogenic sources. Source apportionment using cluster analysis and PCA reveals multiple contributing factors. Non-combustion traffic emissions and industrial activities are identified as dominant sources, supplemented by contributions from combustion processes and crustal dust. Air masses from continental pathways, particularly from the NE, are associated with higher HM concentrations, while southwesterly marine trajectories correspond to cleaner conditions. These findings highlight the combined impacts of local anthropogenic sources and regional transport on deposition patterns in the city. Ecological risk assessment emphasizes the disproportionate role of Pb. Although Zn dominates in terms of concentration and flux, its ecological risk index is low. In contrast, Pb exhibits a high ecological risk compared to other HMs, accounting for nearly 60% of the total PER. This finding indicates Pb is the most critical pollutant of concern in rainwater at HCMC, requiring enhanced emission control strategies. Overall, this study establishes the first quantitative assessment of HM deposition in southern Vietnam under a tropical monsoon climate. Our results address a significant data gap in SEA, where atmospheric deposition measurements remain scarce. These findings enhance the mechanistic understanding of HM deposition in humid monsoon systems and provide a scientific basis for pollution control strategies across rapidly urbanizing regions of SEA.

Conflicts of interest

There are no conflicts to declare.

Data availability

The data supporting the findings of this study are available from the corresponding author upon reasonable request.

Supplementary information (SI) is available. See DOI: https://doi.org/10.1039/d6ea00039h.

Acknowledgements

This research is funded by Vietnam National University, Ho Chi Minh City (VNU-HCM) under grant number C2024-18-24.

During the preparation of this work, the authors used ChatGPT in order to check the English writing. After using this tool, the authors reviewed and edited the content as needed and take full responsibility for the content of the publication.

References

1 P. K. Rai, S. S. Lee, M. Zhang, Y. F. Tsang and K. H. Kim, Heavy metals in food crops: Health risks, fate, mechanisms, and management, *Environ. Int.*, 2019, **125**, 365–385, DOI: 10.1016/j.envint.2019.01.067.

2 N. Sarwar, M. Imran, M. R. Shaheen, W. Ishaque, M. A. Kamran, A. Matloob and S. Hussain, Phytoremediation strategies for soils contaminated with heavy metals: Modifications and future perspectives, *Chemosphere*, 2017, **171**, 710–721, DOI: 10.1016/j.chemosphere.2016.12.116.

3 W. Feng, Z. Guo, C. Peng, X. Xiao, L. Shi, P. Zeng and Q. Xue, Atmospheric bulk deposition of heavy metal(loid)s in central south China: Fluxes, influencing factors and implication for paddy soils, *J. Hazard. Mater.*, 2019, **371**, 634–642, DOI: 10.1016/j.jhazmat.2019.02.090.

4 X. Q. Han, X. Y. Xiao, Z. H. Guo, Y. H. Xie, H. W. Zhu, C. Peng and Y. Q. Liang, Release of cadmium in contaminated paddy soil amended with NPK fertilizer and lime under water management, *Ecotoxicol. Environ. Saf.*, 2018, **159**, 38–45, DOI: 10.1016/j.ecoenv.2018.04.049.

5 X. Ma, Z. Sha, Y. Li, R. Si, A. Tang, A. Fangmeier and X. Liu, Temporal-spatial characteristics and sources of heavy metals in bulk deposition across China, *Sci. Total Environ.*, 2024, **926**, 171903, DOI: 10.1016/j.scitotenv.2024.171903.

6 L. S. P. Nguyen, T. T. L. Do, T. G. H. Vo, Q. H. Le and T. T. Hien, The source and distribution of heavy metals in the atmosphere across Southeast Asia, in *Heavy Metal Remediation*, Springer, Cham, 2024, DOI: 10.1007/978-3-031-53688-5_1.

7 S. L. Tian, Y. P. Pan and Y. S. Wang, Size-resolved source apportionment of particulate matter in urban Beijing during haze and non-haze episodes, *Atmos. Chem. Phys.*, 2016, **16**, 1–19, DOI: 10.5194/acp-16-1-2016.

8 W. Phairuang, P. Suwattiga, S. Hongtieab, M. Inerb, M. Furuuchi and M. Hata, Characteristics, sources, and health risks of ambient nanoparticles ($PM_{0.1}$) bound metal in Bangkok, Thailand, *Atmos. Environ.:X*, 2021, **12**, 100141.

9 L. S. P. Nguyen, L. Zhang, D. W. Lin, N. H. Lin and G. R. Sheu, Eight-year dry deposition of atmospheric mercury to

a tropical high mountain background site downwind of the East Asian continent, *Environ. Pollut.*, 2019, **255**, 113128, DOI: 10.1016/j.envpol.2019.113128.

10 H. Tutun, Y. Aluç, H. A. Kahraman, S. Sevin, M. Yipel and H. Ekici, The content and health risk assessment of selected elements in bee pollen and propolis from Turkey, *J. Food Compos. Anal.*, 2022, **105**, 104234, DOI: 10.1016/j.jfca.2021.104234.

11 G. R. Mostafaii, Z. Bakhtyari, F. Atoof, M. Baziar and N. Mirzaei, Health risk assessment and source apportionment of heavy metals in atmospheric dustfall in a city of Khuzestan Province, Iran, *J. Environ. Health Sci. Eng.*, 2021, **19**, 585–601, DOI: 10.1007/s40201-021-00630-z.

12 Y. D. Ma, Y. Q. Tang, H. Xu, X. Y. Zhang, H. L. Liu, S. Q. Wang and W. T. Zhang, Bulk and wet deposition of trace metals to rural, industrial, and urban areas in the Yangtze River Delta, China, *Ecotoxicol. Environ. Saf.*, 2019, **169**, 185–191, DOI: 10.1016/j.ecoenv.2018.11.002.

13 S. Adhikari, C. Zeng, F. Zhang, N. P. Adhikari, J. Gao, N. Ahmed and M. H. R. Khan, Atmospheric wet deposition of trace elements in Bangladesh: Spatiotemporal variability and source apportionment, *Environ. Res.*, 2023, **217**, 114729, DOI: 10.1016/j.envres.2022.114729.

14 B. A. Begum and P. K. Hopke, Identification of sources from chemical characterization of fine particulate matter and assessment of ambient air quality in Dhaka, Bangladesh, *Aerosol Air Qual. Res.*, 2019, **19**, 118–128, DOI: 10.4209/aaqr.2017.12.0604.

15 Z. Cong, S. Kang, Y. Zhang and X. Li, Atmospheric wet deposition of trace elements to the central Tibetan Plateau, *Appl. Geochem.*, 2010, **25**, 1415–1421, DOI: 10.1016/j.apgeochem.2010.06.011.

16 L. S. P. Nguyen and G. R. Sheu, Four-year measurements of wet mercury deposition at a tropical mountain site in central Taiwan, *Aerosol Air Qual. Res.*, 2019, **19**, 2043–2055, DOI: 10.4209/aaqr.2019.05.0250.

17 Y. Chen, J. Qu, S. Sun, Q. Shi, H. Feng, Y. Zhang and S. Cao, Health risk assessment of total exposure from cadmium in South China, *Chemosphere*, 2021, **269**, 128673, DOI: 10.1016/j.chemosphere.2020.128673.

18 Y. P. Pan and Y. S. Wang, Atmospheric wet and dry deposition of trace elements at ten sites in Northern China, *Atmos. Chem. Phys.*, 2015, **15**, 951–972, DOI: 10.5194/acp-15-951-2015.

19 Y. Liu, F. Xu, W. Liu, X. Liu and D. Wang, Characteristics, sources, exposure and health effects of heavy metals in atmospheric particulate matter, *Curr. Pollut. Rep.*, 2025, **11**, 16, DOI: 10.1007/s40726-025-00344-y.

20 H. L. Liu, J. Zhou, M. Li, Y. M. Hu, X. L. Liu and J. Zhou, Bioavailability of heavy metals from atmospheric deposition in a soil–pakchoi system, *J. Hazard. Mater.*, 2019, **362**, 9–16, DOI: 10.1016/j.jhazmat.2018.09.032.

21 H. Peng, Y. Chen, L. Weng, J. Ma, Y. Ma, Y. Li and M. S. Islam, Comparison of heavy metal input inventories in agricultural soils of North and South China, *Sci. Total Environ.*, 2019, **660**, 776–786, DOI: 10.1016/j.scitotenv.2019.01.066.

22 F. A. Nicholson, S. R. Smith, B. J. Alloway, S. C. Carlton and S. R. Smith, Inventory of heavy metal inputs to agricultural soils in England and Wales, *Sci. Total Environ.*, 2003, **311**, 205–219, DOI: 10.1016/S0048-9697(03)00139-6.

23 Y. Pan, J. Liu, L. Zhang, J. Cao, J. Hu, S. Tian and W. Xu, Bulk deposition and source apportionment of atmospheric heavy metals in rural Beijing, *Atmosphere*, 2021, **12**, 283, DOI: 10.3390/atmos12020283.

24 T. T. Hien, N. D. T. Chi, N. T. Nguyen, L. X. Vinh, N. Takenaka and D. H. Huy, Current status of PM2.5 in Ho Chi Minh City, *Aerosol Air Qual. Res.*, 2019, **19**, 2239–2251, DOI: 10.4209/aaqr.2018.12.0471.

25 T. T. Hien, L. S. P. Nguyen, M. T. Truong, T. D. H. Pham, T. A. Ngan, T. H. Minh and N. T. Nguyen, Spatiotemporal variations of atmospheric mercury in Southern Vietnam, *Atmos. Environ.*, 2024, **333**, 120664, DOI: 10.1016/j.atmosenv.2024.120664.

26 N. D. Dat, V. T. Nguyen, T. D. H. Vo, X. T. Bui, M. H. Bui, L. S. P. Nguyen and C. Lin, Heavy metal contamination in street dust of Southern Vietnam, *Environ. Sci. Pollut. Res.*, 2021, **28**, 50405–50419, DOI: 10.1007/s11356-021-14246-1.

27 L. S. P. Nguyen, T. T. Hien, M. T. Truong, N. D. T. Chi and G. R. Sheu, Atmospheric particulate-bound mercury in a Southeast Asian megacity, *Chemosphere*, 2022, **307**, 135707, DOI: 10.1016/j.chemosphere.2022.135707.

28 V. T. Nguyen, N. D. Dat, T. D. H. Vo, D. H. Nguyen, T. B. Nguyen, L. S. P. Nguyen and X. T. Bui, Characteristics and health risks of metals in highway street dust in Vietnam, *Atmosphere*, 2021, **12**, 1548, DOI: 10.3390/atmos12121548.

29 M. T. Truong, L. S. P. Nguyen, T. T. Hien, T. D. H. Pham and T. T. L. Do, Source apportionment and risk estimation of heavy metals in PM10 in Southern Vietnam, *Aerosol Air Qual. Res.*, 2022, **22**, 220094, DOI: 10.4209/aaqr.220094.

30 L. S. P. Nguyen, T. D. H. Pham, M. T. Truong and A. N. Tran, Characteristics of total gaseous mercury in a tropical megacity and cyclone influence, *Atmos. Pollut. Res.*, 2023, **14**, 101813, DOI: 10.1016/j.apr.2023.101813.

31 A. B. Liyandeniya, M. P. Deeyamulla and N. Priyantha, Source apportionment of rainwater chemistry in Sri Lanka, *Air Qual., Atmos. Health*, 2020, **13**, 1497–1504, DOI: 10.1007/s11869-020-00903-w.

32 T. Navrátil, J. Rohovec, J. Shanley, Š. Matoušková, T. Nováková, A. H. Šmejkalová and R. Prokeš, Atmospheric mercury deposition during industrial phase-out, *Environ. Sci. Pollut. Res.*, 2023, **30**, 123586–123602, DOI: 10.1007/s11356-023-30784-2.

33 G. R. Sheu and N. H. Lin, Wet mercury deposition to a remote islet in the Northwest Pacific, *Atmos. Environ.*, 2013, **77**, 474–481, DOI: 10.1016/j.atmosenv.2013.05.038.

34 R. R. Draxler and G. D. Rolph, *HYSPLIT Model Access via NOAA ARL READY*, NOAA Air Resources Laboratory, 2013.

35 Y. Q. Wang, X. Y. Zhang and R. R. Draxler, TrajStat: GIS-based trajectory statistical analysis software, *Environ. Model. Software*, 2009, **24**, 938–939, DOI: 10.1016/j.envsoft.2009.01.004.

36 P. K. Hopke, Factor and correlation analysis of multivariate environmental data, in *Methods of Environmental Data Analysis*, Springer, Dordrecht, 1992, pp. 139–180, DOI: 10.1007/978-94-011-2920-6_4.
37 N. D. Dat, L. S. P. Nguyen, T. D. H. Vo, T. V. Nguyen, T. T. L. Do, A. T. K. Tran and N. T. T. Hoang, Heavy metal pollution characteristics of road dust in Vietnam, *Environ. Geochem. Health*, 2023, **45**, 7889–7907, DOI: 10.1007/s10653-023-01696-4.
38 X. Querol, M. Viana, A. Alastuey, F. Amato, T. Moreno, S. Castillo, J. Pey, J. De la Rosa, A. S. De La Campa, B. Artíñano and P. Salvador, Source origin of trace elements in PM from regional background, urban and industrial sites of Spain, *Atmos. Environ.*, 2007, **41**, 7219–7231, DOI: 10.1016/j.atmosenv.2007.05.022.
39 R. D. Gawhane, P. S. P. Rao, K. Budhavant, D. C. Meshram and P. D. Safai, Anthropogenic fine aerosols over Pune, India, *Meteorol. Atmos. Phys.*, 2019, **131**, 1497–1508, DOI: 10.1007/s00703-018-0653-y.
40 T. T. Hien, N. D. T. Chi, D. H. Huy, H. A. Le, D. E. Oram, G. L. Forster and A. R. Baker, Soluble trace metals in PM2.5 in Vietnam, *Atmos. Environ.:X*, 2022, **15**, 100178, DOI: 10.1016/j.aeaoa.2022.100178.
41 J. Guo, S. Kang, J. Huang, Q. Zhang, L. Tripathee and M. Sillanpää, Seasonal variation of trace elements in precipitation in Lhasa, *Atmos. Res.*, 2015, **153**, 87–97, DOI: 10.1016/j.atmosres.2014.07.030.
42 M. K. Ninu, M. V. Prasanna and H. Vijith, Trace metals in rainwater of coastal Borneo cities, *Asian J. Atmos. Environ.*, 2021, **15**, 2021076, DOI: 10.5572/AJAE.2021.076.
43 J. E. Kim, Y. J. Han, P. R. Kim and T. M. Holsen, Factors influencing wet deposition of trace elements in rural Korea, *Atmos. Res.*, 2012, **116**, 185–194, DOI: 10.1016/j.atmosres.2012.04.013.
44 T. Blazina, A. Laderach, G. D. Jones, H. Sodemann, H. Wernli, J. W. Kirchner and L. H. Winkel, Marine productivity as a source of trace elements in deposition, *Environ. Sci. Technol.*, 2017, **51**, 108–118, DOI: 10.1021/acs.est.6b03063.
45 D. Vlasov, I. D. Eremina, N. E. Kosheleva, G. Shinkareva, N. E. Chubarova and N. S. Kasimov, Hazardous elements in atmospheric precipitation in Moscow, *Geography, Environment, Sustainability*, 2024, **17**, 70–84, DOI: 10.24057/2071-9388-2024-3408.
46 S. Adhikari, F. Zhang, N. P. Adhikari, C. Zeng, R. R. Pant, K. Ram and M. A. Ahsan, Wet deposition of major ions and nitrogen in Bangladesh, *Atmos. Res.*, 2021, **250**, 105414, DOI: 10.1016/j.atmosres.2020.105414.
47 M. S. Rahman, S. Kumar, M. Nasiruddin and N. Saha, Origin of Cu, Pb and Zn in school dust of Dhaka, *Environ. Sci. Pollut. Res.*, 2021, **28**, 40808–40823, DOI: 10.1007/s11356-021-13565-7.
48 L. Tripathee, J. Guo, S. Kang, R. Paudyal, C. M. Sharma, J. Huang and M. Sillanpää, Mercury and trace elements in wet deposition in Central Himalaya, *Atmos. Res.*, 2020, **234**, 104691, DOI: 10.1016/j.atmosres.2019.104691.
49 B. Liu, S. Kang, J. Sun, Y. Zhang, R. Xu, Y. Wang and Z. Cong, Wet precipitation chemistry at a high-altitude Tibetan site, *Environ. Sci. Pollut. Res.*, 2013, **20**, 5013–5027, DOI: 10.1007/s11356-012-1379-x.
50 T. Wei, Z. Dong, S. Kang, C. Zong, M. Rostami and Y. Shao, Trace element deposition in snowpacks of Tibetan glaciers, *Sci. Total Environ.*, 2019, **689**, 754–764, DOI: 10.1016/j.scitotenv.2019.06.455.
51 Y. P. Pan, X. Y. Zhu, S. L. Tian, L. L. Wang, G. Z. Zhang, Y. B. Zhou and Y. S. Wang, Wet deposition and scavenging during extreme rainstorm events, *Atmos. Ocean. Sci. Lett.*, 2017, **10**, 348–353, DOI: 10.1080/16742834.2017.1343084.
52 F. Cereceda-Balic, M. de la Gala-Morales, R. Palomo-Marin, X. Fadic, V. Vidal, M. Funes and E. Pinilla-Gil, Rainwater chemistry and industrial impact in Chile, *Atmos. Pollut. Res.*, 2020, **11**, 99–109, DOI: 10.1016/j.apr.2020.03.003.
53 Y. C. Lin, S. C. Hsu, C. C. K. Chou, R. Zhang, Y. Wu, S. J. Kao and Y. T. Huang, Trace metal fingerprints of winter haze in Beijing, *Environ. Pollut.*, 2016, **208**, 284–293, DOI: 10.1016/j.envpol.2015.07.044.
54 L. Ye, M. Huang, B. Zhong, X. Wang, Q. Tu, H. Sun and M. Chang, Wet and dry deposition fluxes of heavy metals in Pearl River Delta Region (China): Characteristics, ecological risk assessment, and source apportionment, *J. Environ. Sci.*, 2018, **70**, 106–123, DOI: 10.1016/j.jes.2017.11.019.
55 H. H. Duong, C. D. T. Nguyen, P. L. S. Nguyen and H. T. To, PM2.5 temporal variation in Ho Chi Minh City, *J. Nat. Sci.*, 2018, **2**, 130–137, DOI: 10.32508/stdjns.v2i5.788.
56 P. Liu, Q. Wu, W. Hu, K. Tian, B. Huang and Y. Zhao, Atmospheric deposition effects on soil heavy metal accumulation, *Environ. Pollut.*, 2023, **330**, 121740, DOI: 10.1016/j.envpol.2023.121740.
57 L. A. C. Teixeira, J. P. L. Queiroz and C. Marquez-Sarmiento, Oxidative precipitation of manganese from dilute waters, *Mine Water Environ.*, 2017, **36**, 452–456, DOI: 10.1007/s10230-016-0411-7.
58 X. Wang, B. Ren, Y. Zhou and X. Shi, Manganese release from waste ore under rainfall leaching, *Environ. Sci. Pollut. Res.*, 2022, **29**, 5541–5551, DOI: 10.1007/s11356-021-16081-w.
59 S. Sundriyal, T. Shukla, L. Tripathee and D. P. Dobhal, Natural versus anthropogenic trace elements in Himalayan precipitation, *Environ. Sci. Pollut. Res.*, 2020, **27**, 3462–3472, DOI: 10.1007/s11356-019-07102-w.
60 I. Cheng, A. Al Mamun and L. Zhang, Atmospheric wet deposition of particulate elements: A synthesis review, *Environ. Rev.*, 2021, **29**, 340–353, DOI: 10.1139/er-2020-0118.
61 M. B. B. Karşı, S. Yenısoy-Karakaş and D. Karakaş, Washout and rainout processes in sequential rain samples, *Atmos. Environ.*, 2018, **190**, 53–64, DOI: 10.1016/j.atmosenv.2018.07.018.
62 L. S. P. Nguyen and T. T. Hien, Long-range atmospheric mercury transport to Southern Vietnam, *Bull. Environ. Contam. Toxicol.*, 2024, **112**, 14, DOI: 10.1007/s00128-023-03806-9.
63 A. Samontha, W. Waiyawat, J. Shiowatana and R. G. McLaren, Atmospheric deposition of metals

associated with air particulate matter: fractionation of particulate-bound metals using continuous-flow sequential extraction, *ScienceAsia*, 2007, **33**, 421–428, DOI: 10.2306/scienceasia1513-1874.2007.33.421.

64 H. Z. Tian, Y. Wang, Z. G. Xue, K. Cheng, Y. P. Qu, F. H. Chai and J. M. Hao, Emissions of Hg, As and Se from coal combustion in China, *Atmos. Chem. Phys.*, 2010, **10**, 11905–11919, DOI: 10.5194/acp-10-11905-2010.

65 C. T. Dung, T. Miwa, H. Sato and T. Morikawa, Passenger car and motorcycle fleet characteristics in Vietnam, *Journal of the Eastern Asia Society for Transportation Studies*, 2015, **11**, 890–905, DOI: 10.11175/easts.11.890.

66 Q. B. Tran, L. S. P. Nguyen, N. X. Cuong, T. H. Nguyen, T. X. Vu, L. Q. Hau and N. D. Dat, Road dust heavy metal pollution in urban–industrial transition zones, *Int. J. Environ. Res.*, 2025, **19**, 1–22, DOI: 10.1007/s41742-025-00848-x.

67 B. A. Begum, P. K. Hopke and A. Markwitz, Fine particulate matter air pollution in Bangladesh, *Atmos. Pollut. Res.*, 2013, **4**, 75–86, DOI: 10.5094/APR.2013.008.

68 M. Santoso, D. D. Lestiani and A. Markwitz, Characterization of roadside particulate matter in Jakarta, *J. Radioanal. Nucl. Chem.*, 2013, **297**, 165–169, DOI: 10.1007/s10967-012-2350-5.

69 F. Sannoh, Z. Fatmi, D. O. Carpenter, M. Santoso, A. Siddique, K. Khan and H. A. Khwaja, Air pollution and health impacts in a Southeast Asian megacity, *Sci. Total Environ.*, 2024, **942**, 173403, DOI: 10.1016/j.scitotenv.2024.173403.

70 B. Tang, H. Xu, F. Song, H. Ge and S. Yue, Effects of heavy metals on soil microorganisms in lead–zinc tailings, *Environ. Res.*, 2022, **207**, 112174, DOI: 10.1016/j.envres.2021.112174.

71 C. Beţianu, P. Cozma and M. Gavrilescu, Human health hazards from lead bioaccumulation, in *Lead Toxicity Mitigation: Sustainable Nexus Approaches*, Springer, Cham, 2024, pp. 73–123, DOI: 10.1007/978-3-031-46146-0_5.

72 M. I. Szynkowska, A. Pawlaczyk and E. Maćkiewicz, Bioaccumulation and biomagnification of trace elements in the environment, in *Recent Advances in Trace Elements*, 2018, pp. 251–276, DOI: 10.1002/9781119133780.ch13.